Cancer Cell
Article

Macrophage Binding to Receptor VCAM-1 Transmits Survival Signals in Breast Cancer Cells that Invade the Lungs

Qing Chen,[1] Xiang H.-F. Zhang,[1] and Joan Massagué[1,2,*]
[1]Cancer Biology and Genetics Program
[2]Howard Hughes Medical Institute
Memorial Sloan-Kettering Cancer Center, New York, NY 10065, USA
*Correspondence: j-massague@ski.mskcc.org
DOI 10.1016/j.ccr.2011.08.025

SUMMARY

Aberrant expression of vascular cell adhesion molecule-1 (VCAM-1) in breast cancer cells is associated with lung relapse, but the role of VCAM-1 as a mediator of metastasis has remained unknown. We report that VCAM-1 provides a survival advantage to breast cancer cells that infiltrate leukocyte-rich microenvironments such as the lungs. VCAM-1 tethers metastasis-associated macrophages to cancer cells via counter-receptor α4-integrins. Clustering of cell surface VCAM-1, acting through Ezrin, triggers Akt activation and protects cancer cells from proapoptotic cytokines such as TRAIL. This prosurvival function of VCAM-1 can be blocked by antibodies against α4-integrins. Thus, newly disseminated cancer cells expressing VCAM-1 can thrive in leukocyte-rich microenvironments through juxtacrine activation of a VCAM-1–Ezrin-PI3K/Akt survival pathway.

INTRODUCTION

Primary tumors can release a large number of cells into the circulation long before the tumor is diagnosed and removed. Although distant relapse may eventually occur, the limited number of metastatic lesions that emerge suggests that only a small proportion of the cells that leave a primary tumor succeed at infiltrating, surviving, and ultimately overtaking a distant organ (Fidler, 2003; MacDonald et al., 2002). Recent progress in metastasis research has led to the identification of genes and mechanisms that mediate cancer cell extravasation (Bos et al., 2009; Gupta et al., 2007; Padua et al., 2008; Ricono et al., 2009). Other recently identified metastasis genes directly participate in the ultimate colonization of the invaded organs, an event that may take place after a latency period lasting months or decades depending on the type of cancer (Jones et al., 2006; Kang et al., 2003; Müller et al., 2001; Pàez-Ribes et al., 2009; Yin et al., 1999). However, less is known about the mechanisms that allow the survival of cancer cells immediately upon entering a distant organ and being exposed to an often lethal microenvironment. Cell death upon infiltration of a distant organ is regarded as the single-most important bottleneck for the establishment of distant metastases (Cameron et al., 2000; Luzzi et al., 1998; Wong et al., 2001). To cope with the newly invaded tissue, cancer cells that leave the circulation must interact with the newfound stroma and obtain crucial survival and viability signals. A better understanding of these survival mechanisms is needed for the development of therapeutic strategies to target disseminated cancer cells (DTCs) and thereby eliminate residual disease after the removal of a primary tumor.

The mechanisms that mediate metastasis depend, in part, on organ-specific determinants (Fidler, 2003; Nguyen et al., 2009). For example breast cancer metastasis may affect the lungs, bones, liver, and brain (Anan et al., 2010), organs that present distinct barriers to the entry and survival of circulating cancer cells (CTCs). To have a certain probability of entering these

Significance

Interactions with the stroma are key for the survival of disseminated cancer cells (DTCs) and the development of metastasis. The identification of these mechanisms is essential for the development of strategies to target DTCs. The leukocyte receptor VCAM-1 is aberrantly expressed in lung metastatic breast cancer cells and is shown here to transduce prosurvival signals when engaged by macrophages. As a result, VCAM-1 primes metastatic cells for survival and outgrowth in the leukocyte-rich lung parenchyma microenvironment. The interaction between leukocyte α4-integrins and VCAM-1 in endothelial cells is a validated target in diseases of rampant leukocyte recruitment. Targeting this interaction in VCAM-1$^+$ breast cancer cells renders these cells vulnerable to proapoptotic signals.

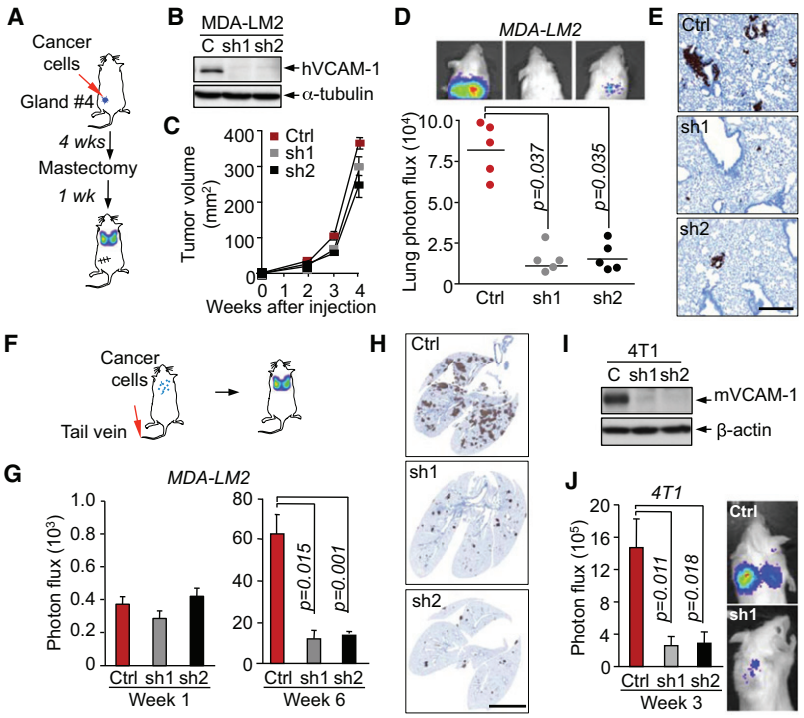

Figure 1. VCAM-1 in Cancer Cells Enhances Lung Metastasis

(A–E) Role of cancer cell VCAM-1 in lung metastasis by mammary tumors. (A) Schematic of the experimental procedure. (B) VCAM-1 protein levels were detected by western immunoblotting in control MDA231-LM2 cells (Ctrl) or these cells expressing independent shRNAs targeting human *VCAM1* (sh1 and sh2).

(C) The indicated cancer cells were injected into the fourth mammary fat pad of mice. Mammary tumor size was measured at the indicated times.

(D) Quantification of lung metastasis at week 5 based on bioluminescent signal.

(E) Lung sections (week 5) were immunostained with human vimentin. Data are average ± SEM; n = 5 mice. Scale bar, 100 μm.

(F–J) Role of cancer cell VCAM-1 in lung colonization from the circulation. (F) Schematic of lung colonization assay by intravenous injection of cancer cells. (G) Indicated MDA231-LM2 cells were intravenously injected into NOD/SCID mice. Lung colonization was quantified by BLI. (H) Representative images of human vimentin staining of lung sections 6 weeks after MDA-231 cell injection. (I) VCAM-1 protein level as detected by western immunoblotting in control 4T1 cells (Ctrl) or these cells expressing independent shRNAs targeting mouse *VCAM1* (sh1 and sh2). 4T1 cells were intravenously injected into BALB/c mice, and lung colonization was quantified by BLI 3 weeks after inoculation. Data are average ± SEM; n = 5 mice. Scale bar, 500 μm.

See also Figure S1.

tissues and resisting the new microenvironment, CTCs must already be primed for infiltration and survival as they leave the source tumor. Based on this line of reasoning, genes that prime cancer cells for survival in a distant organ may be found among gene sets whose expression in primary tumors is clinically associated with distant relapse.

To search for mediators of metastasis that would fulfill these criteria, we focused on an 18 gene lung metastasis signature (LMS) that is expressed in breast cancer cells. The LMS is associated with pulmonary relapse in patients and with lung metastasis in experimental models (Minn et al., 2005). Several LMS genes, including *epiregulin*, *ptgs2*, *mmp1*, *fascin1*, and *angiopoietin-like 4*, mediate extravasation of CTCs by inducing vascular permeability, transendothelial migration, or endothelial cell disjunction (Gupta et al., 2007; Kim et al., 2009; Padua et al., 2008). Notably, the LMS 18 gene set also includes vascular cell adhesion molecule-1 (*vcam1*). VCAM-1 encodes a leukocyte adhesion molecule whose normal expression is restricted to endothelial cells and subpopulations of bone marrow cells (Osborn et al., 1989). Endothelial VCAM-1 binds to the leukocyte integrins α4β1 (or VLA4) and α4β7 on circulating monocytes, granulocytes, and lymphocytes, and tethers these cells to the luminal endothelium surface (Elices et al., 1990; Osborn et al., 1989). Through these interactions, VCAM-1 mediates the movement of leukocytes from blood to tissue, a process that is particularly active during inflammatory responses (Elices et al., 1990; Osborn et al., 1989). Abnormal expression of VCAM-1 has been reported in various cancer cell types, including breast, gastric, renal carcinoma, and melanomas (Ding et al., 2003; Minn et al., 2007; Ruco et al., 1996; Shin et al., 2006). However, the role of VCAM-1 in cancer progression remains unclear. Therefore, we set out to determine whether VCAM-1 in circulating breast cancer cells participates in the infiltration of these cells into distant tissues or their survival in the newly invaded microenvironment.

RESULTS

VCAM-1 Expression in Breast Cancer Cells Enhances Lung Metastasis

VCAM1 emerged as a gene whose expression is associated with the propensity of hormone receptor-negative breast tumors to relapse to the lungs (Minn et al., 2005). In order to investigate whether VCAM-1 functions as a mediator of metastasis, we used short hairpin RNA interference (shRNA) to stably reduce its expression in a VCAM-1-overexpressing lung metastatic cell line, MDA231-LM2-4175 (MDA231-LM2 for short) (Figure 1B; see Figure S1A available online). MDA231-LM2 was obtained by in vivo enrichment for lung metastatic clones from the parental cell line MDA-MB-231 (MDA231 for short) (Minn et al., 2005), which in turn was established from the pleural fluid of a patient with metastatic breast cancer (Cailleau et al., 1974). MDA231 corresponds to the hormone receptor-negative, claudin-low subtype of breast cancer (Prat et al., 2010). Control or VCAM-1-depleted MDA231-LM2 (5×10^5 cells) was implanted in the mammary glands of immunodeficient mice and subjected to a metastasis assessment protocol (Figure 1A). VCAM-1 depletion did not significantly alter the growth rate of the resulting mammary tumors (Figure 1C) or the number of CTCs in the tumor-bearing mice (Figure S1C). However, VCAM-1 depletion decreased by nearly 10-fold the lung metastatic activity of the mammary tumors, as determined by quantitative

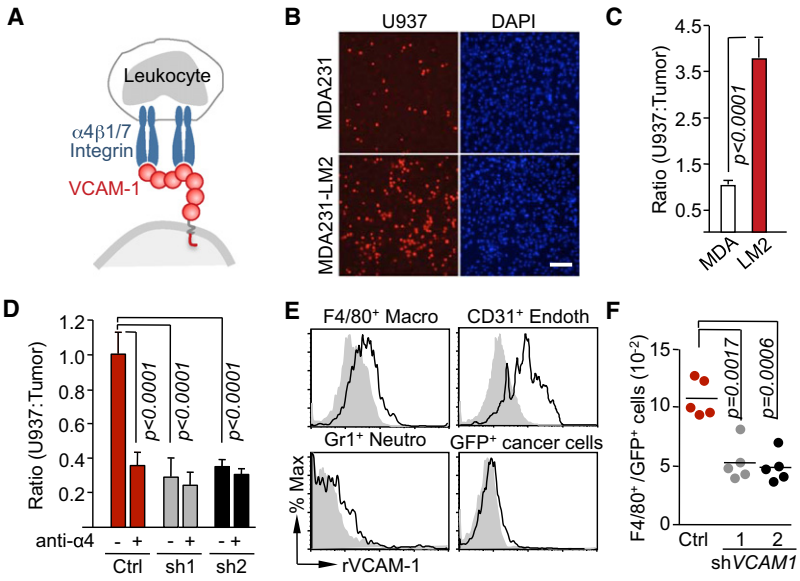

Figure 2. VCAM-1 on Cancer Cells Binds Tumor-Associated Macrophages

(A) Schematic illustration of VCAM-1 interactions with leukocyte α4-integrins.

(B and C) Adhesion assays of U937 cells on monolayers of parental MDA231 or MDA231-LM2 cells. (B) Representative photomicrographs of adherent TRITC-labeled U937 cells on the monolayer of indicated cancer cells. Scale bar, 100 μm. (C) Quantification of the ratio of adherent U937 cells and cancer cells. Data are average ± SEM; n = 10 unit areas.

(D) U937 cells treated with anti-α4-integrin antibody (anti-α4) or Ig control (–) were tested for binding to monolayers of control or *VCAM1*-depleted MDA231-LM2. VCAM-1 knockdown was done using two independent shRNAs (sh1, sh2). Data are average ± SEM; n = 10 unit areas.

(E) rVCAM-1 binging assay with different stromal cell populations from lung metastatic nodules, including F4/80$^+$ macrophages (Macro), Gr-1$^+$ neutrophils (Neutro), and CD31$^+$ endothelial cells (Endoth) and GFP$^+$ cancer cells. Cell surface binding of bovine serum albumin control (gray closed histogram) or rVCAM-1 (black open histogram) was determined by flow cytometry.

(F) Adhesion assays of stromal cells from lung metastatic nodules on monolayers of control or *VCAM1*-depleted (sh1, sh2) MDA231-LM2 cells. The ratio between adherent F4/80$^+$ macrophages to GFP$^+$ cancer cells was quantified by flow cytometry.

See also Figure S2.

bioluminescence imaging (BLI) of an integrated luciferase gene (Figure 1D) or by antihuman vimentin immunohistochemistry (Figure 1E). In a tail vein inoculation protocol to assess lung colonization by a synchronous influx of CTCs (Figure 1F), VCAM-1 depletion did not affect the accumulation of MDA231-LM2 in the lungs during the first week after inoculation (Figure 1G). However, VCAM-1 depletion significantly inhibited the subsequent development of metastatic colonies (Figures 1G and 1H).

To probe the role and significance of VCAM-1 in breast cancer metastasis in a syngeneic, immunocompetent model, we investigated 4T1 breast cancer cells. 4T1 is a lung metastatic cell line derived from a mammary tumor that spontaneously emerged in BALB/c mice (Aslakson and Miller, 1992). Western immunoblotting and qRT-PCR analysis demonstrated that 4T1 cells express VCAM-1 (Figure 1I; Figure S1B). These data show that lung metastatic cells from a spontaneous mouse mammary tumor shared with the human breast cancer counterparts the remarkable feature of expressing this leukocyte-binding endothelial cell receptor. Furthermore, shRNA-mediated depletion of VCAM-1 in 4T1 cells (Figure 1I; Figure S1B) severely inhibited the lung metastatic activity of these cells in immunocompetent BALB/c mice (Figure 1J).

VCAM-1 Mediates Binding of Tumor-Associated Macrophages to Cancer Cells

The extracellular region of VCAM-1 consists of seven immunoglobulin (Ig) domains, one of which (domain 4) is missing in the VCAM-1-6D splice variant (Cybulsky et al., 1991). α4-Integrins bind to separate sites on Ig domains 1 and 4 (Figure 2A), and therefore, the VCAM-1-6D variant is of low affinity (Vonderheide et al., 1994). By means of isoform-specific RT-PCR, we determined that MDA231 and another human metastatic breast cancer cell model, CN34 (see below), predominantly express the long, high-affinity VCAM-1 variant (Figure S2A). To determine whether VCAM-1 on breast cancer cells can bind leukocytes, we incubated MDA231 monolayers with a suspension of U937 cells, a human monocyte cell line that expresses α4β1-integrin (Kalogeris et al., 1999). The MDA231-LM2 cells bound over 3-fold as many U937 cells as did the parental MDA231 cells (Figures 2B and 2C). shRNA-mediated depletion of VCAM-1 in MDA231-LM2 cells or addition of a blocking antibody against α4-integrin inhibited the binding of U937 cells (Figure 2D). We concluded that VCAM-1 on cancer cells can bind monocytes.

Monocytic cells including macrophages enhance tumor progression (Joyce and Pollard, 2009; Qian and Pollard, 2010). Blockage of macrophage recruitment significantly decreases lung colonization by MDA231-LM2 cells in mice (Qian et al., 2009, 2011). However, the specific contribution of macrophages to metastatic colonization is not well understood. To identify metastasis stromal cell types that bind VCAM-1, we generated lung metastatic nodules by tail vein inoculation of MDA231-LM2 cells expressing green fluorescent protein (GFP). Single-cell suspensions prepared from the resulting nodules were incubated with fluorochrome-conjugated recombinant VCAM-1 ectodomain (rVCAM-1) or bovine serum albumin as a control. Specific cell surface markers were used to identify and quantify different types of stromal cells (Figure S2B). VCAM-1 bound to metastasis-associated CD45$^+$F4/80$^+$ macrophages and CD45$^-$CD31$^+$ vascular endothelial cells, but not to Gr1$^+$ neutrophils or GFP$^+$ cancer cells (Figure 2E). Next, we prepared cell suspensions from lung metastasis nodules, depleted these suspensions of human EpCAM$^+$ cancer cells, and panned the remaining cells over control or VCAM-1-depleted MDA231-LM2 monolayers. Analysis of the monolayer-bound fraction demonstrated VCAM-1-dependent binding of F4/80$^+$ cells to MDA231-LM2 cells (Figure 2F).

In 4T1 lung metastatic nodules, CD45$^+$CD4$^+$ and CD45$^+$CD8$^+$ lymphocytes expressed low levels of cell surface α4-integrin

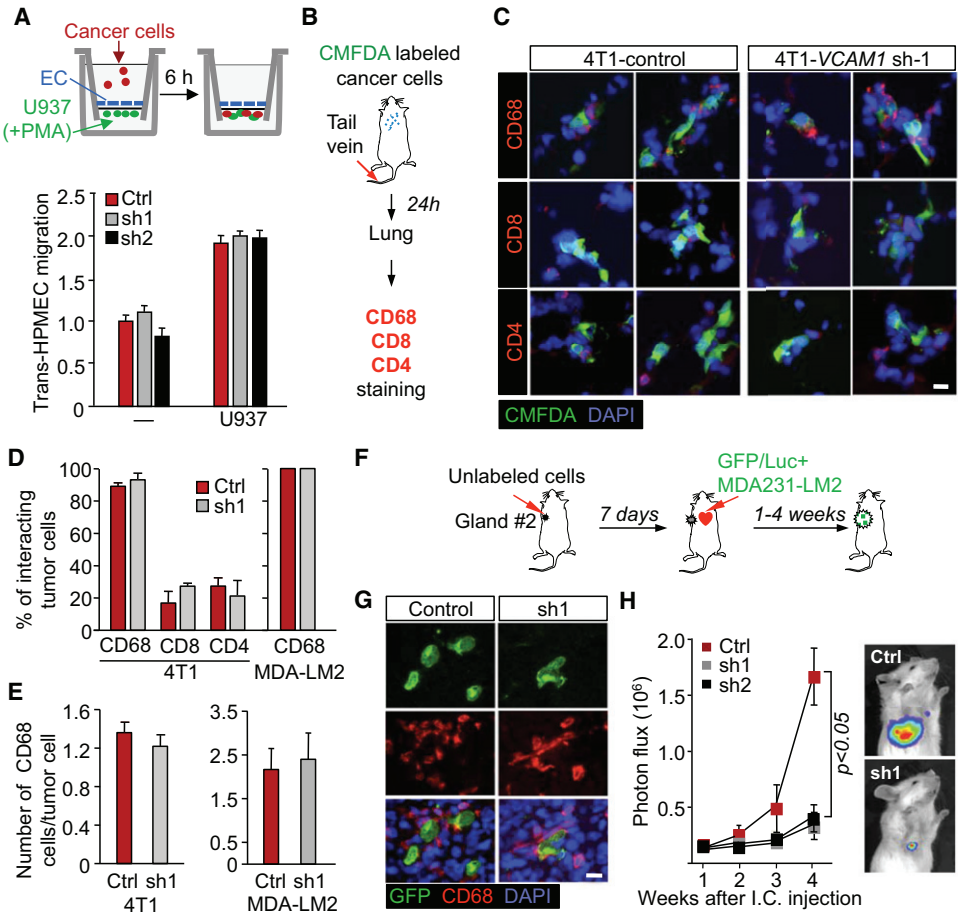

Figure 3. Cancer Cell VCAM-1 Is Dispensable for Transendothelial Migration or Leukocyte Recruitment but Enhances Tumor Seeding

(A) MDA231-LM2 cell migration across monolayers of HPMECs, with or without activated monocytes in the lower chamber of a transwell. Migrated cancer cells were quantified. Data are average ± SEM; n = 10 unit areas.

(B–E) Association of cancer cells with leukocytes in the lungs. (B) Schematic of the experimental procedure. (C) CMFDA-labeled 4T1 cells were intravenously inoculated into BALB/c mice, and the association between cancer cells and $CD4^+$ and $CD8^+$ T cells and $CD68^+$ macrophages was analyzed 24 hr later. Shown are two representative micrographs per experimental group. Scale bar, 10 μm. (D) Percentage of cancer cells interacting with the indicated leukocyte cells. (E) Quantification of $CD68^+$ cells surrounding cancer cells. Data are average ± SEM; n > 30 cancer cells.

(F–H) Tumor self-seeding assay. (F) Schematic of experimental procedure. GFP/luciferase expressing cancer cells of inoculation of into the arterial circulation of mice bearing primary tumors formed by unlabeled cancer cells. (G) Representative images of mammary tumors seeded with indicated GFP^+ MDA-231 LM2 cells. GFP^+ cancer cells and tumor-associated macrophages were stained with anti-GFP and anti-CD68 antibodies in primary tumors (week 4). Scale bar, 10 μm. (H) Seeding of control (Ctrl) or VCAM-1 depleted (sh1 and sh2) MDA231-LM2 cells in mammary tumors after intracardiac inoculation was determined by BLI quantification. Data are average ± SEM; n = 10 mice.

See also Figure S3.

compared to $CD45^+F4/80^+$ macrophages (Figure S2C). Macrophages comprised approximately 7% of the total cell population in the metastatic nodules (Figure S2C), whereas $CD4^+$ and $CD8^+$ lymphocytes collectively comprised 4% of the tumor cell population. Moreover, endothelial cells, which also bind to rVCAM-1 (Figure 2E), comprised <1% of the cell population from MDA231-LM2 lung nodules (Figure S2B). Overall, macrophages were the most abundant source of potential α4-integrin contacts in these lung nodules.

Cancer Cell VCAM-1 Is Dispensable for Extravasation and Macrophage Recruitment

Contacts with macrophages enhance cancer cell extravasation (Qian et al., 2009). Although U937 monocytes enhanced the ability of MDA231-LM2 cells to migrate through human pulmonary microvascular endothelial cell (HPMEC) monolayers, VCAM-1 depletion did not influence this process. This was observed when the monocytes were activated with PMA to induce adherence (Yamamoto et al., 2009) and were placed on the lower side of the transwell membrane (Figure 3A). Similar results were obtained when monocytes stimulated with cyclic-AMP were placed with cancer cells in the upper transwell chamber, with complement factor C5a as a monocyte chemoattractant (Rubin et al., 1991) in the bottom chamber (Figure S3A). VCAM-1 depletion also had no effect when U937 cells were placed together with cancer cells, with CXCL12 as a cancer cell chemoattractant (Zhang et al., 2009) in the bottom chamber (Figure S3B). These results are consistent with our in vivo

evidence that VCAM-1 is not required for entry of breast cancer cells into the lung parenchyma.

To determine if VCAM-1 on cancer cells influenced the recruitment of macrophages into the tumor, we labeled 4T1 or MDA231-LM2 cells with CellTracker Green CMFDA, and inoculated these cells into mice via the tail vein. After 24 hr, we examined the association of $CD4^+$, $CD8^+$ T lymphocytes (for 4T1 model) and $CD68^+$ macrophages (for both 4T1 and MDA231-LM2 models) with $CMFDA^+$ cancer cells in the lung parenchyma (Figures 3B and 3C; Figure S3C). Over 95% of cancer cells were surrounded by macrophages in close juxtaposition, whereas fewer than 30% of cancer cells were associated with $CD4^+$ or $CD8^+$ T lymphocytes (Figure 3D). VCAM-1 depletion in cancer cells changed neither the percentage of cancer cells surrounded by immune cells nor the average number of interacting macrophages per cancer cell (Figures 3D and 3E). Furthermore, the lung nodules formed by the VCAM-1-depleted cells showed the same content of $F4/80^+$, $CD31^+$, and $Gr1^+$ cells as did size-matched control nodules (Figure S2B). Thus, VCAM-1 expression in cancer cells is not required for their recruitment of, or exposure to, macrophages.

VCAM-1 in Cancer Cells Enhances the Seeding of Breast Tumors

We further tested the role of VCAM-1 under conditions that challenged cancer cells to seed new or established tumors. VCAM-1 depletion significantly diminished the rate of tumor outgrowth when only 5×10^4 cells were implanted in mammary fat pad tumor assays (Figures S3D–S3F, compare to tumor formation by 5×10^5 implanted cells in Figure 1C). Recently, we showed in experimental models that established breast tumors are powerful magnets for CTCs (Kim et al., 2009). In this process, called ''self-seeding,'' CTCs that pass through a breast tumor can effectively reinvade the tumor by virtue of their metastatic abilities, the leaky tumor vasculature, and the attraction of inflammatory cytokines IL6 and IL8 in the tumor microenvironment. Once in that environment, aggressive seeder clones can attract myeloid cells through the release of CXCL1 and expand in that myeloid-rich microenvironment (Kim et al., 2009). In a tumor self-seeding assay (Figure 3F), MDA231-LM2 seeder cells were indeed surrounded by $CD68^+$ macrophages (Figure 3G). MDA231 seeder cells that were depleted of VCAM-1 showed a marked decrease in the ability to populate the recipient tumors (Figure 3H). Collectively, these results suggest that VCAM-1 supports the outgrowth of cancer cells that infiltrate the lungs and other restrictive sites. Moreover, these results raised the possibility that VCAM-1-leukocyte interactions are a source of this advantage.

VCAM-1 Protects Breast Cancer Cells from Apoptosis in the Lung Microenvironment

To determine how VCAM-1 expression in breast cancer cells contributes to tumor outgrowth in the lungs, we transduced a doxycycline-driven *VCAM1* shRNA expression system in MDA231-LM2 cells. Doxycycline addition to the culture media decreased *VCAM1* expression within 48 hr, whereas a full recovery of VCAM-1 expression after doxycycline removal took 5 days (Figures 4A and 4B). Cells cultured without doxycycline were inoculated into tail vein, and 1 day after the inoculation, doxycycline was administered to the mice for the remainder of the experiment (Figure 4C). This treatment caused a sustained inhibition of lung metastatic colonization. In a converse experiment, cancer cells were incubated with doxycycline for 3 days in order to suppress VCAM-1 expression prior to inoculation of these cells into mice. The recipient mice were not treated with doxycycline. Metastatic colonization of the lungs under these conditions was as extensive as with control MDA231-LM2 cells (Figure 4D). Therefore, VCAM-1 was dispensable for cancer cell entry into the lungs but was required for their subsequent outgrowth.

VCAM-1 depletion caused a marked increase in the proportion of apoptotic cells in the lung metastatic colonies (Figure 4E). We also observed a high incidence of apoptosis in lung nodules seeded from mammary tumors (Figure 4; refer to protocol in Figure 1B). We saw no effect of VCAM-1 depletion on the expression of the cell proliferation marker Ki67 or the endothelial cell marker CD31 in lung nodules that were either size matched or time matched relative to controls (Figures S4A–S4C). The lesions formed by VCAM-1-depleted cells remained low in VCAM-1 expression compared to size-matched control lesions, as determined by qRT-PCR analysis of lung nodules (Figure S4D). Collectively, the results suggest that VCAM-1 specifically enhances the survival of breast cancer cells that infiltrate the lung parenchyma.

The VCAM-1 Intracellular Domain Mediates Metastatic Cell Survival

We investigated the mechanism underlying this unprecedented role of VCAM-1. We generated a truncated form, VCAM-1(Δcyt), lacking the cytoplasmic region (Figure 5A) and compared this construct with the wild-type VCAM-1 for the ability to restore lung metastatic activity in VCAM-1-depleted cancer cells. In addition to the MDA231-LM2 model system, we also used the CN34-LM2 cell line. This line is a lung metastatic derivative from the pleural fluid of a patient with stage IV metastatic breast cancer (Tavazoie et al., 2008). The VCAM-1 and VCAM-1(Δcyt) constructs were expressed at similar levels in these two cell lines, as determined by immunoblotting analysis (Figure 5B) and flow cytometry (Figure 5C). Both constructs similarly increased the ability of MDA231-LM2 and CN34-LM2 cells to bind U937 monocytes (Figure 5D). However, whereas the expression of wild-type VCAM-1 increased the ability of both cell lines to colonize the lungs (Figure 5E) and to avert apoptosis (Figure 5F), VCAM-1(Δcyt) was defective in these functions in both cell lines (Figures 5E and 5F).

Engagement of VCAM-1 Triggers Survival Signals

The interaction of leukocyte α4-integrin with VCAM-1 induces cytoskeletal rearrangements in endothelial cells, and this effect can be mimicked with the use of anti-VCAM-1 crosslinking antibodies (van Wetering et al., 2003). We adopted this approach to test the effect of VCAM-1 clustering on the apoptotic responsiveness of cancer cells to TRAIL (tumor necrosis factor-related apoptosis-inducing ligand), a proapoptotic cytokine expressed in human lung metastatic nodules (Zhang et al., 2009). In both MDA231-LM2 and CN34-LM2 cell cultures, addition of TRAIL induced the activation of effector caspase-3, as determined by the accumulation of cleaved caspase-3 (Figure 6A) (Nicholson

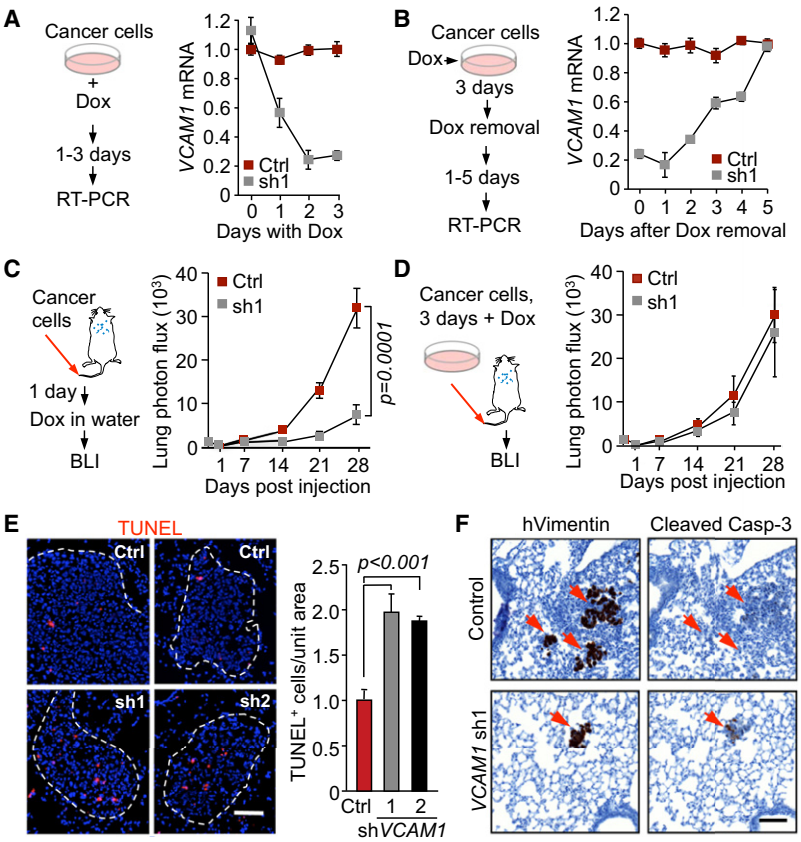

Figure 4. VCAM-1 Protects Cancer Cells from Apoptosis in the Lung Microenvironment

(A and B) MDA231-LM2 cells with a doxycycline (Dox)-inducible shVCAM-1 vector were cultured in the presence of doxycycline (A) or were placed in doxycycline-free medium after culturing with doxycycline (B), in order to determine the kinetics of *VCAM1* depletion and recovery, respectively.

(C) Control or doxycycline-driven *VCAM1* shRNA cells were inoculated into mice, and all mice were treated with doxycycline. Lung colonization was assessed by quantitative BLI.

(D) BLI quantification of lung colonization after the indicated cancer cells pretreated with doxycycline were injected into mice that were not given doxycycline. The mice were not administrated with drug. Data are average ± SEM; n = 8 mice.

(E) TUNEL staining and quantification in the lungs harvested 6 weeks after intravenous injection of cancer cells as indicated in Figure 1E. Representative photomicrographs, and quantification of TUNEL$^+$ cells. Data are average ± SEM; n = 10 unit area/mouse, 3 mice/group. Scale bar, 50 μm.

(F) The indicated cancer cells were injected into the fourth mammary fat pad of mice, and the lungs were harvested as indicated in Figure 1A. Immunostaining for human vimentin and cleaved caspase-3 was performed on consecutive lung tissue sections. Scale bar, 100 μm.

See also Figure S4.

et al., 1995). Incubation with anti-VCAM-1 antibody and secondary F(ab′)$_2$ fragment markedly blunted this effect in the cells expressing full-length VCAM-1, but importantly, not in cells expressing VCAM-1(Δcyt) (Figure 6A).

To determine the effect of engaging VCAM-1 with its natural α4-integrin counter-receptors, we incubated cancer cells with U937 monocytes. Cancer cells expressing VCAM-1, VCAM-1 (Δcyt), or no exogenous VCAM-1 were prelabeled with CMFDA, and apoptosis was assessed by TUNEL staining (Figure 6B). Expression of VCAM-1 reduced to half the incidence of apoptosis in cancer cells that were exposed to TRAIL, whereas VCAM-1(Δcyt) provided no protection (Figure 6C). Furthermore, addition of anti-α4-integrin-blocking antibody prevented VCAM-1 from exerting this antiapoptotic effect (Figure 6C). Cancer cell counts corroborated these findings (Figure 6D). Thus, upon engagement by α4-integrin on leukocytes, VCAM-1 in breast cancer cells delivers antiapoptotic signals via its cytoplasmic tail.

VCAM-1 Clustering Activates Akt Signaling

To identify signaling pathways that are activated by VCAM-1 engagement, we performed antibody-mediated clustering of VCAM-1 in MDA231 and CN34 cells under low concentration of serum growth factors. Cell lysates were probed with phosphopeptide-directed antibodies that detect the activation state of 46 protein kinases and their protein substrates (Phospho-Kinase Array Kit) as well as Smad2/3 and NF-κB (Table S1). Among these signal transducers only Akt phosphorylation at S473 showed a consistent increase in response to VCAM-1 clustering (Table S1). S473 phosphorylation is an Akt-activating event triggered by PI3K stimulation and catalyzed by the TORC2 complex (Alessi et al., 1996; Collins et al., 2003; Sarbassov et al., 2005). S473 phosphorylation by TORC2 is thought to prime Akt for further phosphorylation and activation by 3-phosphoinositide dependent protein kinase 1 (PDK1) at T308 (Zoncu et al., 2011). Using western immunoblotting, we confirmed that VCAM-1 clustering induces Akt phosphorylation at S473 in human MDA231, CN34, and mouse 4T1 breast cancer cells (Figures 7A and 7B). S473 phosphorylation peaked 10–15 min after VCAM-1 clustering. No Akt phosphorylation was detected in MDA231 or CN34 cells expressing VCAM-1(Δcyt) (Figure 7A). Addition of the PI3K inhibitor LY-294002 abolished the induction of Akt phosphorylation by VCAM-1 clustering (Figure 7B). Furthermore, in the presence of LY-294002, VCAM-1 clustering no longer suppressed caspase-3 activation by TRAIL (Figure 7C). Collectively, these results suggest that engagement of VCAM-1 on breast cancer cells triggers activation of the PI3K/Akt pathway and protects cancer cells from death signals.

VCAM-1 Clustering Triggers Akt Binding to Ezrin

The short intracellular tail of VCAM-1 and of intercellular cell adhesion molecules 1–3 (ICAM-1–3) interacts with Ezrin, a member of the ERM (Ezrin/Radixin/Moesin) protein family (Fehon et al., 2010). ERM proteins are cytoplasmic proteins that function as a link between certain transmembrane proteins and the actin cytoskeleton (Fehon et al., 2010). In endothelial cells the

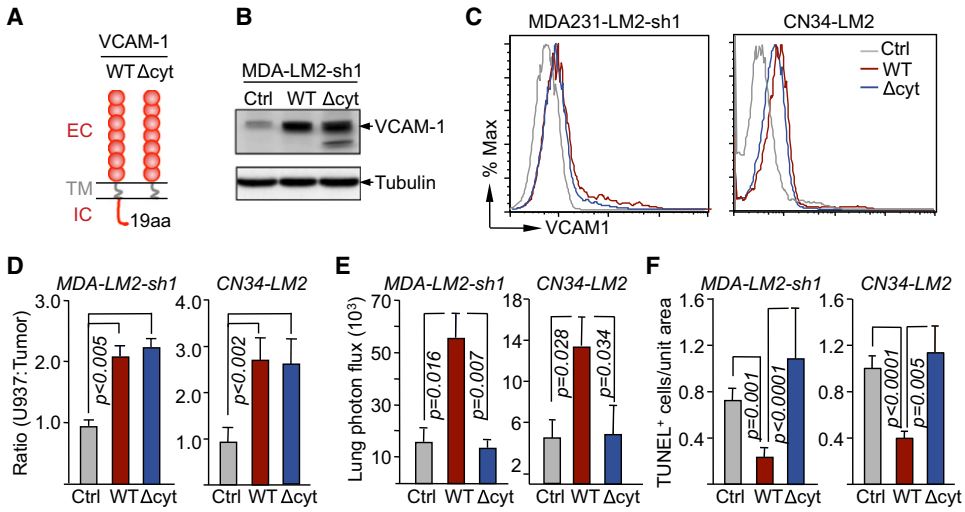

Figure 5. The VCAM-1 Intracellular Domain Mediates Survival of Cancer Cells in the Lungs

(A) Domain structure of the wild-type (WT) VCAM-1 with extracellular (EC), transmembrane (TM), and intracellular (IC) domains and VCAM-1 (ΔCyt) construct lacking the IC. WT or ΔCyt VCAM-1 was overexpressed in *VCAM1*-depleted (by shRNA 1) MDA231-LM2 cells (MDA-LM2-sh1) and CN34-LM2 cells.

(B and C) Expression of the wild-type VCAM-1, VCAM-1(ΔCyt), or empty vector (Ctrl) in MDA231-LM2 cells that were stably depleted of endogenous VCAM-1 by the expression of shRNA1 and CN34-LM2 cells. (B) VCAM-1 was detected by western immunoblotting in MDA231-LM2 cells. (C) The expression of VCAM-1 on the cell surface was detected by flow cytometry.

(D) U937 cell adhesion assays on monolayers of the indicated MDA231 or CN34 cell lines. Data are average ± SEM; n = 10 unit areas.

(E and F) The indicated cell lines were intravenously injected into mice. Six weeks after tumor cell injection, lung BLI was measured (E), and TUNEL$^+$ cells were quantified in lung tissue sections (F). Data are average ± SEM; n = 5 mice.

interaction of VCAM-1 with Ezrin triggers cytoskeletal rearrangements for the translocation of VCAM-1-bound leukocytes from blood into tissue (Barreiro et al., 2002; van Wetering et al., 2003). In addition to this role, Ezrin can signal cell survival through the PI3K pathway (Gautreau et al., 1999). Antibody-mediated crosslinking of ICAM-2 triggers phosphorylation of Ezrin at Y353, which results in binding and activation of PI3K (Perez et al., 2002). Y353 is located within the α-helical domain of Ezrin, and Y353 phosphorylation is thought to indirectly involve Src kinases (Chuan et al., 2006; Krieg and Hunter, 1992). Based on these clues, we hypothesized that VCAM-1 engagement may trigger Akt activation though Ezrin. Indeed, antibody-mediated clustering of VCAM-1 in MDA231-LM2 or CN34 cells in low-serum conditions led to a rapid phosphorylation of Ezrin at Y353 (Figure 7D). VCAM-1(Δcyt) failed to mediate this effect (Figure 7D). Moreover, this effect was accompanied by the formation of a complex between Ezrin and Akt (Figure 7D) and an enhanced recruitment of Akt to the membrane (Figure 7E; Figure S5). The results suggest that VCAM-1 signaling activates Ezrin Y353 phosphorylation to help PI3K recruit Akt to the membrane, leading to TORC2 activation of Akt signaling (summarized in Figure 7F).

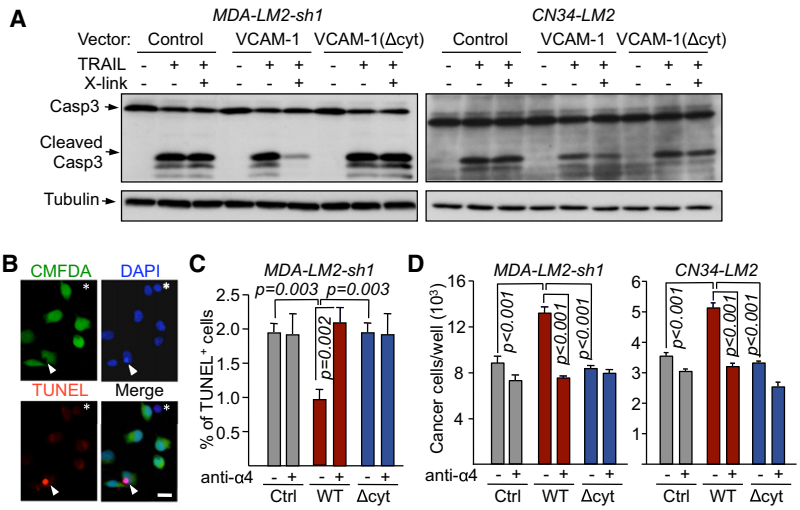

Figure 6. VCAM-1 Engagement by α4-Integrins Triggers Antiapoptotic Signals via the Cytoplasmic Domain

(A) VCAM-1 clustering antibodies (Ab X-linking) were added to the indicated cell lines in the presence or absence of 10 ng/ml TRAIL for 3 hr. Caspase-3 activation was detected by western immunoblotting.

(B–D) The indicated cancer cells were cocultured with U937 cells in the presence of TRAIL and α4-integrin antibody (anti-α4) or comparable Ig control (−). (B) After 24 hr, TUNEL$^+$ (red) and Green CMFDA-labeled cancer cells were scored under a fluorescent microscope. Arrowheads indicate a TUNEL$^+$/CMFDA$^+$ cancer cell, and asterisks indicate a (CMFDA-negative) U937 cell. (C) Percentage of TUNEL$^+$/CMFDA$^+$ cancer cells. Data are average ± SEM; n = 10 unit areas; p value calculated using t test. Scale bar, 20 μm. (D) Cancer cells were quantified after 48 hr of coculture. Data are average ± SEM; n = 4 samples.

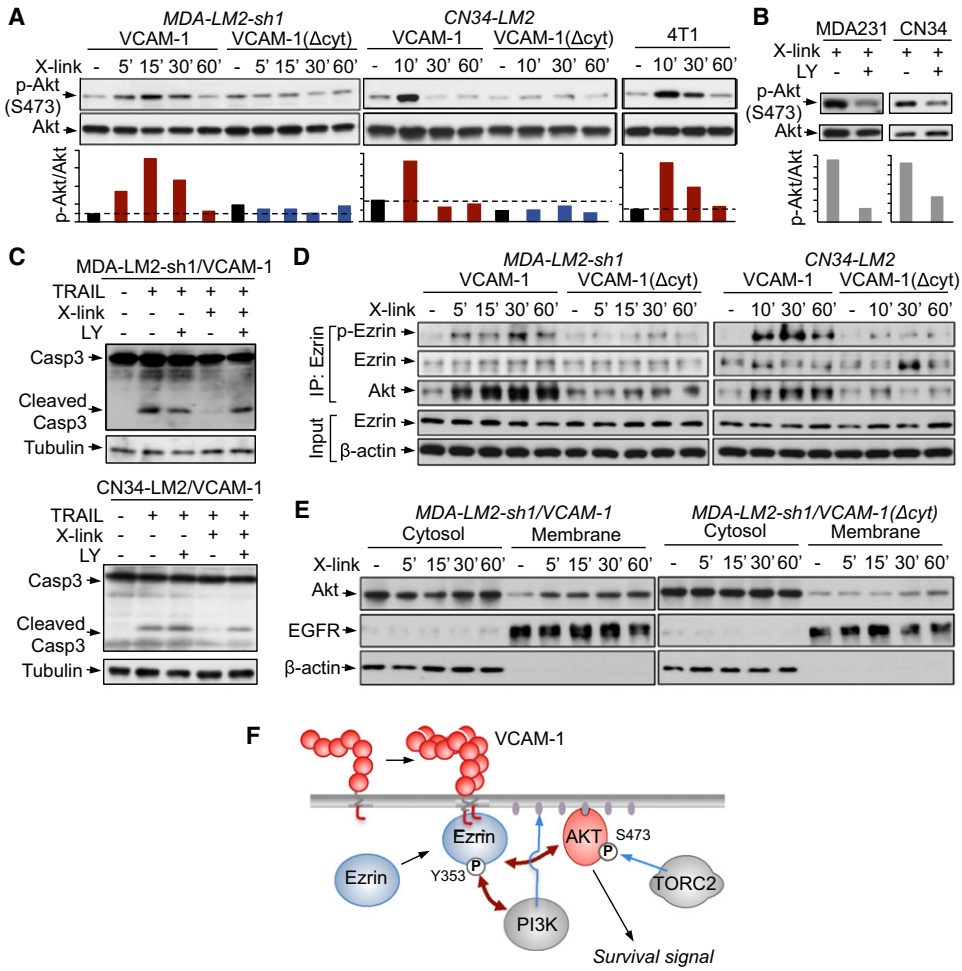

Figure 7. VCAM-1 Clustering Activates PI3K/Akt Signaling with the Involvement of Ezrin

(A) Time course of Akt phosphorylation at the TORC2 site S473 after addition of VCAM-1 clustering antibodies. The indicated human MDA-231 and CN34 and mouse 4T1 breast cancer cells were used in low-serum media. The ratio of phospho-Akt to total Akt is shown below each lane.

(B) Cancer cells overexpressing VCAM-1 were pretreated with PI3K inhibitor LY294002 (LY) or vehicle DMSO (–) for 30 min. VCAM-1 antibody clustering was applied for 10 min, and activated Akt (S473) was detected by western blotting. The ratio of phospho-Akt to Akt is shown below each lane.

(C) Cancer cells overexpressing VCAM-1 were pretreated with LY294002 (LY) or vehicle (–) for 30 min, and VCAM-1 clustering antibodies and TRAIL (10 ng/ml) were added for 3 hr as indicated. Caspase-3 activation was detected by western immunoblotting.

(D) Time course of Ezrin phosphorylation at Y353 and Ezrin-Akt interaction after addition of VCAM-1 clustering antibodies to the indicated cells. The indicated proteins were analyzed by western immunoblotting of whole-cell lysates (Input) or anti-Ezrin immunoprecipitates (IP: Ezrin).

(E) Time course of Akt association with the cell membrane fraction after addition of VCAM-1 clustering antibodies to the indicated cells. Immunoblotting with antibodies against EGFR and β-actin served as markers of membrane and cytosolic fractions, respectively.

(F) Model of VCAM-1-mediated Akt activation. VCAM-1 clustering triggers Ezrin phosphorylation at Y353, which is a known docking site for PI3K. This event is accompanied by Akt binding to Ezrin, Akt association with the cell membrane, and Akt phosphorylation at the TORC2 site S473 for propagation of survival signals.

See also Figure S5 and Table S1.

VCAM-1 Association with Leukocyte-Rich Breast Tumors and Metastases

Unlike the lung metastatic populations derived from the MDA231 and CN34 parental cell lines, brain metastatic and bone metastatic populations that we isolated from these same sources (Bos et al., 2009; Minn et al., 2005) did not show elevated expression of *VCAM1* (Figure 8A). This phenomenon was noteworthy in the case of the brain metastatic derivatives, which otherwise share various organ infiltrative genes and function with the lung metastatic counterparts (Bos et al., 2009). To investigate the association in human tissue material, we determined the *VCAM1* transcript level in lung, brain, and bone metastasis samples from patients with breast cancer (Figure 8B). The results demonstrated a significantly higher expression of VCAM-1 in the lung and bone metastases compared to the brain metastases (Figure 8B). There was no correlation between the expression of *VCAM1* and that of the vascular endothelial marker *CD31* in metastasis tissues (Figure S6A), arguing that the level of *VCAM1* expression was not a reflection of the endothelial cell content of the metastatic lesions. The bone marrow is rich with α4-integrin-expressing hematopoietic cells. Paradoxically, the overexpression of VCAM-1 in MDA231 (Figures S6B and S6C)

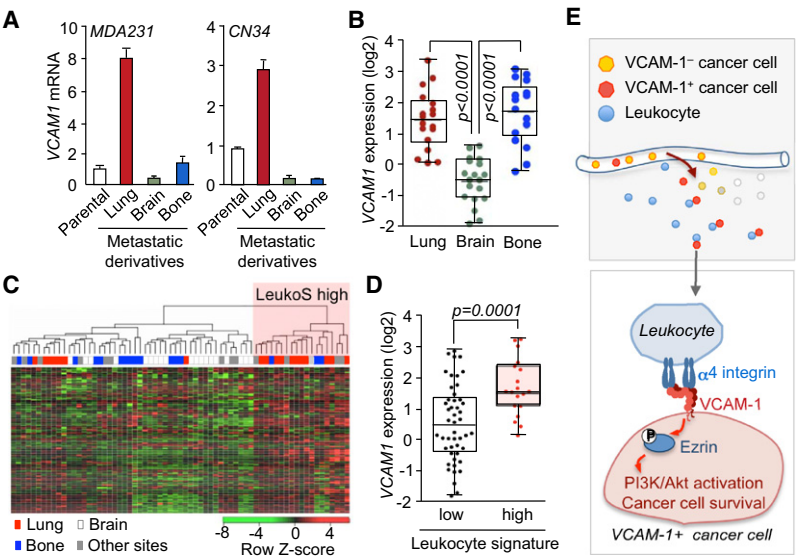

Figure 8. *VCAM1* Expression Is Associated with Leukocyte Content in Breast Tumors

(A) Relative *VCAM1* mRNA level in lung metastatic, brain metastatic, and bone metastatic cells derived from parental MDA231 or CN34 cell lines. Data are average ± SEM; n = 3.

(B) *VCAM1* expression in metastatic tissues from patients with cancer including samples from lung (n = 18), brain (n = 19), and bone metastasis (n = 17).

(C and D) *VCAM1* expression in metastatic lesions with high or low leukocyte content. (C) Clustering of 67 metastatic samples of patients with breast cancer by LeukoS. (D) *VCAM1* expression in leukocyte signature high and low clusters of metastatic lesions.

(E) Model of the survival advantage obtained by breast cancer cells that express VCAM-1 in leukocyte-rich tissues such as the lung. On exposure to macrophages and other leukocytes, the engagement of VCAM-1 by α4-integrin counter-receptors triggers Ezrin phosphorylation and activation of PI3K/Akt signaling. PI3K/Akt signaling opposes the effects of death cytokines in the pulmonary microenvironment.

See also Figure S6.

did not enhance the ability of these cells to initiate bone marrow colonization (Figures S6D–S6F).

The selective association of *VCAM1* expression with lung metastasis was intriguing in light of our functional evidence linking stromal leukocytes and VCAM-1-mediated cancer cell survival. Therefore, we sought evidence for a possible association of *VCAM1* expression with the leukocyte content of primary tumors. From a gene expression signature of $CD45^{+}CD10^{-}$ leukocytes isolated from human breast tumors (Allinen et al., 2004), we generated a bioinformatic classifier. Using this tool, we classified 67 metastasis tissue samples from patients with breast cancer into leukocyte gene expression signature (LeukoS)-high and -low groups (Figure 8C). The LeukoS-high group was highly enriched for lung metastasis samples and excluded most of the bone and brain metastasis samples (Figure 8C). This finding is consistent with the natural capacity of the lung parenchyma to be infiltrated by lymphoid and myeloid cells (Lipscomb et al., 1995). Furthermore, a comparison of the *VCAM1* transcript levels with the leukocyte signature score of these tumors revealed that *VCAM1* expression was enriched in the LeukoS-high metastases (Figure 8D). These results with clinical samples are consistent with the implication from our functional studies that VCAM-1-expressing cancer cells have a survival advantage to initiate metastasis at sites that are rich in leukocytes, such as the lungs (Figure 8E).

DISCUSSION

The adaptation of newly arrived cancer cells to the microenvironment of distal organs is a stringent rate-limiting step in metastasis, and the probability of completing this step varies widely depending on the tumor type and the target organ. The specific stromal interactions that dictate the compatibility of DTCs with a particular organ site have remained largely a mystery. Focusing on VCAM-1 as an overexpressed gene in breast cancer cells that preferentially colonize the lungs, we show that this cell adhesion molecule is engaged by counter-receptor α4-integrins on leukocytes to trigger PI3K/Akt activation and cancer cell survival in the pulmonary parenchyma (Figure 8E). Our findings provide a biochemical explanation for the clinical association of VCAM-1 expression in breast tumors with cancer relapse to the lungs (Minn et al., 2005). Our findings also show that VCAM-1 expression is high in leukocyte-rich lung metastasis samples from patients with breast cancer compared to brain metastasis samples. We propose that these associations are based on a prosurvival advantage provided by VCAM-1 in cancer cells that invade leukocyte-rich sites such as the lungs.

Tumor-associated macrophages and other stromal leukocytes play crucial roles in various aspects of tumorigenesis through the secretion of specific cytokines and proteases (Cheng et al., 2007; Giraudo et al., 2004; Gocheva et al., 2010; Lin et al., 2006; Sangaletti et al., 2008; Wyckoff et al., 2004). The present results reveal an unprecedented role for juxtacrine stimulation of cancer cells by macrophages during metastatic colonization. VCAM-1 on the surface of cancer cells mediates α4-integrin-dependent binding of macrophages, and its oligomerization triggers PI3K/Akt signaling in the cancer cells. High-resolution imaging techniques recently demonstrated physical contacts between macrophages and breast cancer cells during macrophage-facilitated CTC extravasation in mice (Qian et al., 2009). However, we found no contribution of VCAM-1 to cancer cell extravasation or macrophage recruitment into tumors. Rather, our evidence suggests that the α4-integrin-VCAM-1 interaction promotes cancer cell survival through PI3K/Akt pathway activation by the VCAM-1 cytoplasmic domain. During leukocyte transmigration, VCAM-1 on endothelial cells can communicate with the cytoplasmic proteins Ezrin and Moesin, and trigger Rac1 activation (Barreiro et al., 2002; van Wetering et al., 2003). Our data indicate that VCAM-1 clustering in breast cancer cells mediates Ezrin phosphorylation, Akt binding to Ezrin, and Akt phosphorylation at the TORC2 site S473 to activate prosurvival signaling. The protein kinase(s) responsible for Ezrin phosphorylation at Y353 remains unknown, although Src has been implicated as an indirect mediator (Chuan et al.,

2006; Krieg and Hunter, 1992). Thus, leukocyte engagement of VCAM-1 in breast cancer cells may serve to amplify the activation of the PI3K/Akt pathway in a mitogen-poor microenvironment during the initial stages of seeding and adaptation of DTCs to new sites.

We propose that VCAM-1 expression confers breast cancer cells with a selective survival advantage in leukocyte-rich tissues. As organs exposed to the outside environment, the lungs are rich in resident immune cells (Lipscomb et al., 1995). In tumor-bearing mice the lungs accumulate bone marrow-derived mononuclear phagocytes and endothelial progenitors, cell types that express α4-integrins (Gao et al., 2008; Kaplan et al., 2005). Our data suggest that α4-integrin-expressing leukocytes and endothelial cells in lungs mediate Akt prosurvival signaling by directly interacting with VCAM-1 in metastatic breast cancer cells. The pulmonary parenchyma thereby provides a matching receptive soil for CTCs that express VCAM-1, explaining the observed link between VCAM-1 expression in primary tumors and selective relapse to the lungs (Minn et al., 2005).

Cancer cells departing from a breast tumor with high expression of VCAM-1 would be primed for survival in the leukocyte-rich microenvironment of the lungs. In comparison the brain has a limited presence of microglial macrophages, which is in line with the lack of an association of VCAM-1 with brain metastasis that we observed. In the case of bone metastasis, we found no association between VCAM-1 expression in primary tumors and bone relapse, and no effect of VCAM-1 overexpression on the ability of breast cancer cells to initiate bone marrow colonization in mice. VCAM-1 may not provide an early advantage in the bone marrow because Akt activation in cancer cells that enter this site can be provided by other mechanisms, such as Src-dependent CXCL12 signaling (Zhang et al., 2009). We do not rule out a role of VCAM-1 later in the osteolytic phase of bone metastasis.

What drives the selection for VCAM-1-expressing cancer cells in breast tumors is unknown, but it is possible that VCAM-1-rich clones are positively selected in breast tumor areas of active infiltration or inflammation. Macrophage-rich areas of a primary tumor would nurture the expansion of VCAM-1-expressing cancer cell clones. Furthermore, breast cancer cells in lung metastatic nodules can reenter the circulation, seed back a mammary tumor, and abundantly proliferate in leukocyte-rich tumor areas (Kim et al., 2009), and we provide evidence that VCAM-1 favors the outgrowth of CTCs that infiltrate a self-seeding mammary tumor. Accordingly, lung metastatic clones expressing VCAM-1 might undergo recurrent cycles of amplification by shuttling between lung nodules and a leukocyte-rich primary tumor microenvironment.

By disrupting the α4-integrin-VCAM-1 interaction between macrophages and cancer cells with anti-α4-integrin-blocking antibodies, we were able to cancel the prosurvival action of VCAM-1 in the cancer cells. The interaction between endothelial VCAM-1 and leukocyte α4-integrins is a validated target in multiple sclerosis and other diseases that involve rampant recruitment of circulating leukocytes into tissue (Comi, 2009; Schmidt et al., 2009). Our results point at a potential application of such targeted drugs to suppress VCAM-1-mediated survival of DTCs after the removal of a primary tumor.

EXPERIMENTAL PROCEDURES

Animal Studies

All experiments using animals were done in accordance to a protocol approved by MSKCC Institutional Animal Care and Use Committee (IACUC). Female NOD/SCID or BALB/c mice (NCI; Charles River Lab and Taconic Farm) between 5 and 7 weeks old were used. Lung metastasis assays from orthotopic inoculation followed previously described procedures (Padua et al., 2008). A total of 5×10^5 cancer cells in 50 μl of 1:1 mix of PBS/growth factor-reduced Matrigel (BD Biosciences) was injected into the fourth right mammary fat pad of mice. The primary tumors were surgically removed when they each reached approximately 300 mm^3. After 7 days, lung metastases were quantified using BLI. For lung colonization assays, 2×10^5 cells in 100 μl PBS were intravenously injected, and lung colonization was quantified using BLI. For inducible knockdown experiments, doxycycline hyclate (Sigma-Aldrich) was added into the drinking water (2 mg/ml). For the primary tumor implantation with a low number of cells, 5×10^4 cells were injected. Tumor-seeding assays followed previously described procedures (Kim et al., 2009). A total of 5×10^5 unlabeled MDA231 parental cells were injected into the second right mammary fat pad of mice. After 7 days, 100,000 GFP/luciferase-integrated LM2 cells were intracardially injected into tumor-bearing mice. To detect tumor-immune cell interactions in the lungs, cancer cells were labeled with 5 μM CellTracker Green CMFDA (Molecular Probes), and 10^6 labeled cells were intravenously injected. Lung tissues were harvested 24 hr after injection, and CD4, CD8, and CD68 staining was performed. To detect CTCs, the whole-blood perfusate from tumor-bearing mice was collected, and total RNA was extracted. The relative expression of human β2-microglobulin was assessed by qRT-PCR and normalized to murine β2-microglobulin.

Cell-Cell Binding Assays

A total of 2×10^6 prelabeled U937 cells were allowed to adhere to the monolayer of cancer cells. Adherent cells (red) and the nucleus of total cells (DAPI staining in blue) were scored by fluorescence microscopy. The ratio of adherent U937 cells to cancer cells was calculated as red counts/(blue counts − red counts). In the indicated experiments, U937 cells were preincubated with functional blocking antibody of α4-integrin (10 μg/ml; clone PS/2 from AbD Serotec) or Ig control for 30 min. To identify the cell types that adhere to cancer cells, human EpCAM-depleted stromal cell suspensions from lung metastatic nodules were allowed to adhere to GFP^+ cancer cell monolayers. Single-cell suspensions of cancer cells and adherent cells were incubated with fluorochrome-conjugated F4/80 antibody. $F4/80^+$ macrophages and GFP^+ cancer cells were quantified using flow cytometry.

VCAM-1 Clustering Assays

VCAM-1 in human cancer cells was crosslinked with 10 μg/ml of mouse anti-human VCAM-1 monoclonal antibody (clone 1G11; Beckman Coulter) and 50 μg/ml goat anti-mouse IgG_1 $F(ab')_2$ (Jackson ImmunoResearch) for indicated time frames, whereas 10 μg/ml of mouse anti-human VCAM-1 monoclonal antibody (Clone MVCAM.A429; AbD Serotec) and 50 μg/ml goat anti-rat IgG_1 $F(ab')_2$ (Jackson ImmunoResearch) were used in 4T1 mouse breast cancer cells. Mouse or rat IgG was used as control. For apoptosis analysis, cancer cells were incubated with 100 ng/ml TRAIL (PeproTech) for 3 hr. Caspase-3 was detected by western immunoblotting. To identify signaling mediators, VCAM-1 clustering was performed in serum-starved human breast cancer cells for the indicated time periods. Where indicated, 50 μM LY294002 or DMSO control was added during the incubation with anti-VCAM-1 and $F(ab')_2$. Cell lysates were analyzed using Human Phospho-Kinase Array Kit (R&D Systems). In the indicated experiments, western blot was performed using antibodies against phospho-Akt (S473), Akt, phospho-NF-κB p65 (S468), or phospho-Smad2 (S465/467) and phospho-Smad3 (S423/425) (all from Cell Signaling). The ratio of phospho-Akt to total Akt was quantified by ImageJ software (Abramoff et al., 2004). For coimmunoprecipitation assays, cell pellets were lysed with IP buffer (Pierce). Equal amounts of protein were incubated with anti-Ezrin (clone 3C12; Abcam) and protein G (GE Healthcare). Ezrin, phospho-Ezrin (Y353; BD PharMingen), and Akt were detected in the immunoprecipitates. For cell fractionation, membrane and cytosolic fractions were harvested using Subcellular Protein Fractionation kit

(Pierce). Akt was detected in each fraction, whereas EGFR or β-actin (Cell Signaling) was used as the loading control for membrane or cytosolic fraction, respectively.

To clustering VCAM-1 in tumor cells by physiologically interacting with α4-integrin in macrophages, confluent cancer cells were cocultured with U937 cells (2.5×10^5 U937 cells/cm^2) in the presence of 20 ng/ml TRAIL. To detect the percentage of apoptotic cancer cells, cancer cells were prelabeled with Green CMFDA before the coculture. TUNEL staining was performed 24 hr after incubation and observed under the fluorescent microscope. To quantify survived tumor cells, cells were lysed by Passive Lysis Buffer (Promega), and the luciferase activity was detected by Luciferase Assay System (Promega) using GloMax 96 Microplate Luminometer (Promega). Standard curve was generated by detecting the luciferase activity of a series number of cancer cells, and the absolute number of survived cancer cells was calculated. In the indicated experiments, α4-integrin antibody was applied in the coculture system.

Analysis of Human Metastatic Tissue Samples

VCAM1 transcript level was analyzed in 18 lung, 19 brain, and 17 bone metastatic samples from patients with breast cancer (GSE14020) (Zhang et al., 2009). A correlation coefficient was calculated between *VCAM1* and *CD31* expression in each data set. A LeukoS, including 182 genes, was based on the SAGE data from $CD45^+CD10^-$ leukocytes isolated from breast tumors (Allinen et al., 2004). After mapping these genes on the Affymetrix U133A platform, the probe sets of these genes were queried in a data set from 67 metastatic samples from patients with breast cancer (GSE14020) (Zhang et al., 2009). We clustered all these samples using the *heatmap.2* function in the R statistical package. The most robust subcluster was defined as the leukocyte signature high (LeukoS-high) group. *VCAM1* expressions were compared between these two groups.

Statistical Analysis

Pairwise comparisons were performed by two-tailed Student's t test. Significance was set at p values less than 0.05.

SUPPLEMENTAL INFORMATION

Supplemental Information includes six figures, one table, and Supplemental Experimental Procedures and can be found with this article online at doi:10.1016/j.ccr.2011.08.025.

ACKNOWLEDGMENTS

The authors thank J. Joyce and members of the J.M. lab for insightful discussion and technical suggestions, and the MSKCC Molecular Cytology Core Facility for histological sample staining and analysis. This work was supported by National Institutes of Health Grants CA126518 and CA94060, and the Alan and Sandra Gerry Metastasis Research Initiative. Q.C. is supported by Life Sciences Research Foundation Fellowship. J.M. is an investigator of the Howard Hughes Medical Institute.

Received: January 30, 2011
Revised: July 7, 2011
Accepted: August 17, 2011
Published: October 17, 2011

REFERENCES

Abramoff, M.D., Magelhaes, P.J., and Ram, S.J. (2004). Image processing with ImageJ. Biophotonics International *11*, 36–42.

Alessi, D.R., Andjelkovic, M., Caudwell, B., Cron, P., Morrice, N., Cohen, P., and Hemmings, B.A. (1996). Mechanism of activation of protein kinase B by insulin and IGF-1. EMBO J. *15*, 6541–6551.

Allinen, M., Beroukhim, R., Cai, L., Brennan, C., Lahti-Domenici, J., Huang, H., Porter, D., Hu, M., Chin, L., Richardson, A., et al. (2004). Molecular characterization of the tumor microenvironment in breast cancer. Cancer Cell *6*, 17–32.

Anan, K., Mitsuyama, S., Koga, K., Tanabe, R., Saimura, M., Tanabe, Y., Watanabe, M., Suehara, N., Matsunaga, H., Nishihara, K., et al. (2010). Disparities in the survival improvement of recurrent breast cancer. Breast Cancer *17*, 48–55.

Aslakson, C.J., and Miller, F.R. (1992). Selective events in the metastatic process defined by analysis of the sequential dissemination of subpopulations of a mouse mammary tumor. Cancer Res. *52*, 1399–1405.

Barreiro, O., Yanez-Mo, M., Serrador, J.M., Montoya, M.C., Vicente-Manzanares, M., Tejedor, R., Furthmayr, H., and Sanchez-Madrid, F. (2002). Dynamic interaction of VCAM-1 and ICAM-1 with moesin and ezrin in a novel endothelial docking structure for adherent leukocytes. J. Cell Biol. *157*, 1233–1245.

Bos, P.D., Zhang, X.H., Nadal, C., Shu, W., Gomis, R.R., Nguyen, D.X., Minn, A.J., van de Vijver, M.J., Gerald, W.L., Foekens, J.A., and Massagué, J. (2009). Genes that mediate breast cancer metastasis to the brain. Nature *459*, 1005–1009.

Cailleau, R., Young, R., Olivé, M., and Reeves, W.J., Jr. (1974). Breast tumor cell lines from pleural effusions. J. Natl. Cancer Inst. *53*, 661–674.

Cameron, M.D., Schmidt, E.E., Kerkvliet, N., Nadkarni, K.V., Morris, V.L., Groom, A.C., Chambers, A.F., and MacDonald, I.C. (2000). Temporal progression of metastasis in lung: cell survival, dormancy, and location dependence of metastatic inefficiency. Cancer Res. *60*, 2541–2546.

Cheng, J., Huo, D.H., Kuang, D.M., Yang, J., Zheng, L., and Zhuang, S.M. (2007). Human macrophages promote the motility and invasiveness of osteopontin-knockdown tumor cells. Cancer Res. *67*, 5141–5147.

Chuan, Y.C., Pang, S.T., Cedazo-Minguez, A., Norstedt, G., Pousette, A., and Flores-Morales, A. (2006). Androgen induction of prostate cancer cell invasion is mediated by ezrin. J. Biol. Chem. *281*, 29938–29948.

Collins, B.J., Deak, M., Arthur, J.S., Armit, L.J., and Alessi, D.R. (2003). In vivo role of the PIF-binding docking site of PDK1 defined by knock-in mutation. EMBO J. *22*, 4202–4211.

Comi, G. (2009). Treatment of multiple sclerosis: role of natalizumab. Neurol. Sci. *30* (*Suppl 2*), S155–S158.

Cybulsky, M.I., Fries, J.W., Williams, A.J., Sultan, P., Eddy, R., Byers, M., Shows, T., Gimbrone, M.A., Jr., and Collins, T. (1991). Gene structure, chromosomal location, and basis for alternative mRNA splicing of the human VCAM1 gene. Proc. Natl. Acad. Sci. USA *88*, 7859–7863.

Ding, Y.B., Chen, G.Y., Xia, J.G., Zang, X.W., Yang, H.Y., and Yang, L. (2003). Association of VCAM-1 overexpression with oncogenesis, tumor angiogenesis and metastasis of gastric carcinoma. World J. Gastroenterol. *9*, 1409–1414.

Elices, M.J., Osborn, L., Takada, Y., Crouse, C., Luhowskyj, S., Hemler, M.E., and Lobb, R.R. (1990). VCAM-1 on activated endothelium interacts with the leukocyte integrin VLA-4 at a site distinct from the VLA-4/fibronectin binding site. Cell *60*, 577–584.

Fehon, R.G., McClatchey, A.I., and Bretscher, A. (2010). Organizing the cell cortex: the role of ERM proteins. Nat. Rev. Mol. Cell Biol. *11*, 276–287.

Fidler, I.J. (2003). The pathogenesis of cancer metastasis: the 'seed and soil' hypothesis revisited. Nat. Rev. Cancer *3*, 453–458.

Gao, D., Nolan, D.J., Mellick, A.S., Bambino, K., McDonnell, K., and Mittal, V. (2008). Endothelial progenitor cells control the angiogenic switch in mouse lung metastasis. Science *319*, 195–198.

Gautreau, A., Poullet, P., Louvard, D., and Arpin, M. (1999). Ezrin, a plasma membrane-microfilament linker, signals cell survival through the phosphatidylinositol 3-kinase/Akt pathway. Proc. Natl. Acad. Sci. USA *96*, 7300–7305.

Giraudo, E., Inoue, M., and Hanahan, D. (2004). An amino-bisphosphonate targets MMP-9-expressing macrophages and angiogenesis to impair cervical carcinogenesis. J. Clin. Invest. *114*, 623–633.

Gocheva, V., Wang, H.W., Gadea, B.B., Shree, T., Hunter, K.E., Garfall, A.L., Berman, T., and Joyce, J.A. (2010). IL-4 induces cathepsin protease activity in tumor-associated macrophages to promote cancer growth and invasion. Genes Dev. *24*, 241–255.

Gupta, G.P., Nguyen, D.X., Chiang, A.C., Bos, P.D., Kim, J.Y., Nadal, C., Gomis, R.R., Manova-Todorova, K., and Massagué, J. (2007). Mediators of vascular remodelling co-opted for sequential steps in lung metastasis. Nature *446*, 765–770.

Jones, D.H., Nakashima, T., Sanchez, O.H., Kozieradzki, I., Komarova, S.V., Sarosi, I., Morony, S., Rubin, E., Sarao, R., Hojilla, C.V., et al. (2006). Regulation of cancer cell migration and bone metastasis by RANKL. Nature *440*, 692–696.

Joyce, J.A., and Pollard, J.W. (2009). Microenvironmental regulation of metastasis. Nat. Rev. Cancer *9*, 239–252.

Kalogeris, T.J., Kevil, C.G., Laroux, F.S., Coe, L.L., Phifer, T.J., and Alexander, J.S. (1999). Differential monocyte adhesion and adhesion molecule expression in venous and arterial endothelial cells. Am. J. Physiol. *276*, L9–L19.

Kang, Y., Siegel, P.M., Shu, W., Drobnjak, M., Kakonen, S.M., Cordón-Cardo, C., Guise, T.A., and Massagué, J. (2003). A multigenic program mediating breast cancer metastasis to bone. Cancer Cell *3*, 537–549.

Kaplan, R.N., Riba, R.D., Zacharoulis, S., Bramley, A.H., Vincent, L., Costa, C., MacDonald, D.D., Jin, D.K., Shido, K., Kerns, S.A., et al. (2005). VEGFR1-positive haematopoietic bone marrow progenitors initiate the pre-metastatic niche. Nature *438*, 820–827.

Kim, M.Y., Oskarsson, T., Acharyya, S., Nguyen, D.X., Zhang, X.H., Norton, L., and Massagué, J. (2009). Tumor self-seeding by circulating cancer cells. Cell *139*, 1315–1326.

Krieg, J., and Hunter, T. (1992). Identification of the two major epidermal growth factor-induced tyrosine phosphorylation sites in the microvillar core protein ezrin. J. Biol. Chem. *267*, 19258–19265.

Lin, E.Y., Li, J.F., Gnatovskiy, L., Deng, Y., Zhu, L., Grzesik, D.A., Qian, H., Xue, X.N., and Pollard, J.W. (2006). Macrophages regulate the angiogenic switch in a mouse model of breast cancer. Cancer Res. *66*, 11238–11246.

Lipscomb, M.F., Bice, D.E., Lyons, C.R., Schuyler, M.R., and Wilkes, D. (1995). The regulation of pulmonary immunity. Adv. Immunol. *59*, 369–455.

Luzzi, K.J., MacDonald, I.C., Schmidt, E.E., Kerkvliet, N., Morris, V.L., Chambers, A.F., and Groom, A.C. (1998). Multistep nature of metastatic inefficiency: dormancy of solitary cells after successful extravasation and limited survival of early micrometastases. Am. J. Pathol. *153*, 865–873.

MacDonald, I.C., Groom, A.C., and Chambers, A.F. (2002). Cancer spread and micrometastasis development: quantitative approaches for in vivo models. Bioessays *24*, 885–893.

Minn, A.J., Gupta, G.P., Siegel, P.M., Bos, P.D., Shu, W., Giri, D.D., Viale, A., Olshen, A.B., Gerald, W.L., and Massagué, J. (2005). Genes that mediate breast cancer metastasis to lung. Nature *436*, 518–524.

Minn, A.J., Gupta, G.P., Padua, D., Bos, P., Nguyen, D.X., Nuyten, D., Kreike, B., Zhang, Y., Wang, Y., Ishwaran, H., et al. (2007). Lung metastasis genes couple breast tumor size and metastatic spread. Proc. Natl. Acad. Sci. USA *104*, 6740–6745.

Müller, A., Homey, B., Soto, H., Ge, N., Catron, D., Buchanan, M.E., McClanahan, T., Murphy, E., Yuan, W., Wagner, S.N., et al. (2001). Involvement of chemokine receptors in breast cancer metastasis. Nature *410*, 50–56.

Nguyen, D.X., Bos, P.D., and Massagué, J. (2009). Metastasis: from dissemination to organ-specific colonization. Nat. Rev. Cancer *9*, 274–284.

Nicholson, D.W., Ali, A., Thornberry, N.A., Vaillancourt, J.P., Ding, C.K., Gallant, M., Gareau, Y., Griffin, P.R., Labelle, M., Lazebnik, Y.A., et al. (1995). Identification and inhibition of the ICE/CED-3 protease necessary for mammalian apoptosis. Nature *376*, 37–43.

Osborn, L., Hession, C., Tizard, R., Vassallo, C., Luhowskyj, S., Chi-Rosso, G., and Lobb, R. (1989). Direct expression cloning of vascular cell adhesion molecule 1, a cytokine-induced endothelial protein that binds to lymphocytes. Cell *59*, 1203–1211.

Padua, D., Zhang, X.H., Wang, Q., Nadal, C., Gerald, W.L., Gomis, R.R., and Massagué, J. (2008). TGFbeta primes breast tumors for lung metastasis seeding through angiopoietin-like 4. Cell *133*, 66–77.

Pàez-Ribes, M., Allen, E., Hudock, J., Takeda, T., Okuyama, H., Viñals, F., Inoue, M., Bergers, G., Hanahan, D., and Casanovas, O. (2009). Antiangiogenic therapy elicits malignant progression of tumors to increased local invasion and distant metastasis. Cancer Cell *15*, 220–231.

Perez, O.D., Kinoshita, S., Hitoshi, Y., Payan, D.G., Kitamura, T., Nolan, G.P., and Lorens, J.B. (2002). Activation of the PKB/AKT pathway by ICAM-2. Immunity *16*, 51–65.

Prat, A., Parker, J.S., Karginova, O., Fan, C., Livasy, C., Herschkowitz, J.I., He, X., and Perou, C.M. (2010). Phenotypic and molecular characterization of the claudin-low intrinsic subtype of breast cancer. Breast Cancer Res. *12*, R68.

Qian, B., Deng, Y., Im, J.H., Muschel, R.J., Zou, Y., Li, J., Lang, R.A., and Pollard, J.W. (2009). A distinct macrophage population mediates metastatic breast cancer cell extravasation, establishment and growth. PLoS One *4*, e6562.

Qian, B.Z., and Pollard, J.W. (2010). Macrophage diversity enhances tumor progression and metastasis. Cell *141*, 39–51.

Qian, B.Z., Li, J., Zhang, H., Kitamura, T., Zhang, J., Campion, L.R., Kaiser, E.A., Snyder, L.A., and Pollard, J.W. (2011). CCL2 recruits inflammatory monocytes to facilitate breast-tumour metastasis. Nature *475*, 222–225.

Ricono, J.M., Huang, M., Barnes, L.A., Lau, S.K., Weis, S.M., Schlaepfer, D.D., Hanks, S.K., and Cheresh, D.A. (2009). Specific cross-talk between epidermal growth factor receptor and integrin alphavbeta5 promotes carcinoma cell invasion and metastasis. Cancer Res. *69*, 1383–1391.

Rubin, J., Titus, L., and Nanes, M.S. (1991). Regulation of complement 5a receptor expression in U937 cells by phorbol ester. J. Leukoc. Biol. *50*, 502–508.

Ruco, L.P., de Laat, P.A., Matteucci, C., Bernasconi, S., Sciacca, F.M., van der Kwast, T.H., Hoogsteden, H.C., Uccini, S., Mantovani, A., and Versnel, M.A. (1996). Expression of ICAM-1 and VCAM-1 in human malignant mesothelioma. J. Pathol. *179*, 266–271.

Sangaletti, S., Di Carlo, E., Gariboldi, S., Miotti, S., Cappetti, B., Parenza, M., Rumio, C., Brekken, R.A., Chiodoni, C., and Colombo, M.P. (2008). Macrophage-derived SPARC bridges tumor cell-extracellular matrix interactions toward metastasis. Cancer Res. *68*, 9050–9059.

Sarbassov, D.D., Guertin, D.A., Ali, S.M., and Sabatini, D.M. (2005). Phosphorylation and regulation of Akt/PKB by the rictor-mTOR complex. Science *307*, 1098–1101.

Schmidt, K.J., Büning, J., Jankowiak, C., Lehnert, H., and Fellermann, K. (2009). Crohn's targeted therapy: myth or real goal? Curr. Drug Discov. Technol. *6*, 290–298.

Shin, J., Kim, J., Ryu, B., Chi, S.G., and Park, H. (2006). Caveolin-1 is associated with VCAM-1 dependent adhesion of gastric cancer cells to endothelial cells. Cell. Physiol. Biochem. *17*, 211–220.

Tavazoie, S.F., Alarcón, C., Oskarsson, T., Padua, D., Wang, Q., Bos, P.D., Gerald, W.L., and Massagué, J. (2008). Endogenous human microRNAs that suppress breast cancer metastasis. Nature *451*, 147–152.

van Wetering, S., van den Berk, N., van Buul, J.D., Mul, F.P., Lommerse, I., Mous, R., ten Klooster, J.P., Zwaginga, J.J., and Hordijk, P.L. (2003). VCAM-1-mediated Rac signaling controls endothelial cell-cell contacts and leukocyte transmigration. Am. J. Physiol. Cell Physiol. *285*, C343–C352.

Vonderheide, R.H., Tedder, T.F., Springer, T.A., and Staunton, D.E. (1994). Residues within a conserved amino acid motif of domains 1 and 4 of VCAM-1 are required for binding to VLA-4. J. Cell Biol. *125*, 215–222.

Wong, C.W., Lee, A., Shientag, L., Yu, J., Dong, Y., Kao, G., Al-Mehdi, A.B., Bernhard, E.J., and Muschel, R.J. (2001). Apoptosis: an early event in metastatic inefficiency. Cancer Res. *61*, 333–338.

Wyckoff, J., Wang, W., Lin, E.Y., Wang, Y., Pixley, F., Stanley, E.R., Graf, T., Pollard, J.W., Segall, J., and Condeelis, J. (2004). A paracrine loop between tumor cells and macrophages is required for tumor cell migration in mammary tumors. Cancer Res. *64*, 7022–7029.

Yamamoto, T., Sakaguchi, N., Hachiya, M., Nakayama, F., Yamakawa, M., and Akashi, M. (2009). Role of catalase in monocytic differentiation of U937 cells by TPA: hydrogen peroxide as a second messenger. Leukemia *23*, 761–769.

Yin, J.J., Selander, K., Chirgwin, J.M., Dallas, M., Grubbs, B.G., Wieser, R., Massagué, J., Mundy, G.R., and Guise, T.A. (1999). TGF-beta signaling blockade inhibits PTHrP secretion by breast cancer cells and bone metastases development. J. Clin. Invest. *103*, 197–206.

Zhang, X.H., Wang, Q., Gerald, W., Hudis, C.A., Norton, L., Smid, M., Foekens, J.A., and Massagué, J. (2009). Latent bone metastasis in breast cancer tied to Src-dependent survival signals. Cancer Cell *16*, 67–78.

Zoncu, R., Efeyan, A., and Sabatini, D.M. (2011). mTOR: from growth signal integration to cancer, diabetes and ageing. Nat. Rev. Mol. Cell Biol. *12*, 21–35.